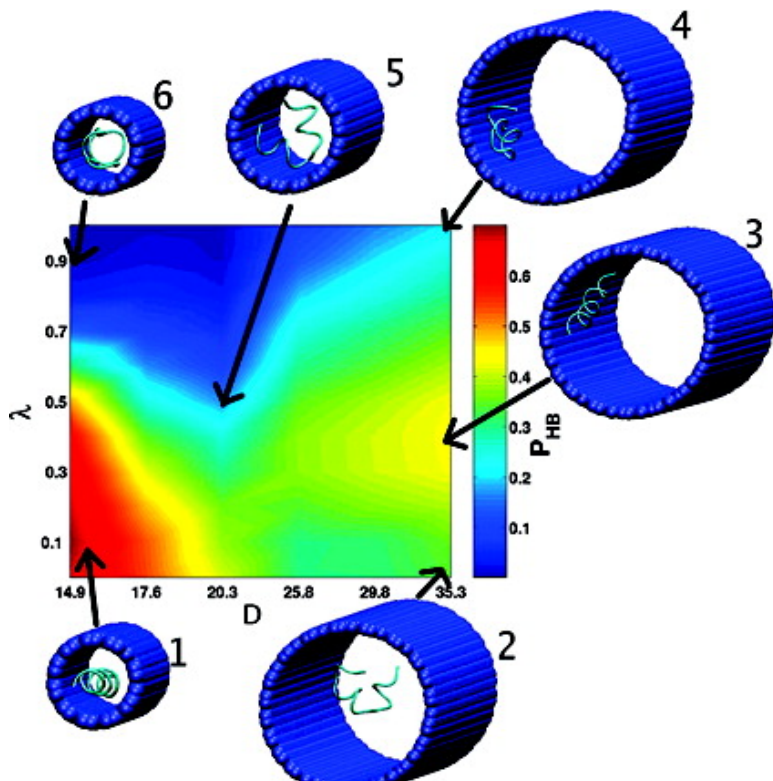


## Factors Governing Helix Formation in Peptides Confined to Carbon Nanotubes

Edward P. O'Brien, George Stan, D. Thirumalai, and Bernard R. Brooks

*Nano Lett.*, 2008, 8 (11), 3702-3708 • DOI: 10.1021/nl8019328 • Publication Date (Web): 26 September 2008

Downloaded from <http://pubs.acs.org> on March 6, 2009



### More About This Article

Additional resources and features associated with this article are available within the HTML version:

- Supporting Information
- Access to high resolution figures
- Links to articles and content related to this article
- Copyright permission to reproduce figures and/or text from this article



ACS Publications

High quality. High impact.

Nano Letters is published by the American Chemical Society. 1155 Sixteenth Street N.W., Washington, DC 20036

# NANO LETTERS

Subscriber access provided by UNIV OF MARYLAND COLL PARK

[View the Full Text HTML](#)



ACS Publications

High quality. High impact.

---

Nano Letters is published by the American Chemical Society. 1155 Sixteenth Street N.W., Washington, DC 20036

# Factors Governing Helix Formation in Peptides Confined to Carbon Nanotubes

Edward P. O'Brien,<sup>†,‡</sup> George Stan,<sup>§</sup> D. Thirumalai,<sup>\*,†,||</sup> and Bernard R. Brooks<sup>‡</sup>

*Biophysics Program, Institute for Physical Science and Technology, University of Maryland, College Park, Maryland 20742, Laboratory of Computational Biology, National Heart Lung and Blood Institute, National Institutes of Health, Bethesda, Maryland 20892, Department of Chemistry, University of Cincinnati, Cincinnati, Ohio 45221, and Department of Chemistry and Biochemistry, University of Maryland, College Park, Maryland 20742*

Received July 2, 2008

## ABSTRACT

The effect of confinement on the stability and dynamics of peptides and proteins is relevant in the context of a number of problems in biology and biotechnology. We have examined the stability of different helix-forming sequences upon confinement to a carbon nanotube using Langevin dynamics simulations of a coarse-grained representation of the polypeptide chain. We show that the interplay of several factors that include sequence, solvent conditions, strength ( $\lambda$ ) of nanotube-peptide interactions, and the nanotube diameter ( $D$ ) determines confinement-induced stability of helices. In agreement with predictions based on polymer theory, the helical state is entropically stabilized for all sequences when the interaction between the peptide and the nanotube is weakly hydrophobic and  $D$  is small. However, there is a *strong* sequence dependence as the strength of the  $\lambda$  increases. For an amphiphilic sequence, the helical stability increases with  $\lambda$ , whereas for polyalanine the diagram of states is a complex function of  $\lambda$  and  $D$ . In addition, decreasing the size of the “hydrophobic patch” lining the nanotube, which mimics the chemical heterogeneity of the ribosome tunnel, increases the helical stability of the polyalanine sequence. Our results provide a framework for interpreting a number of experiments involving the structure formation of peptides in the ribosome tunnel as well as transport of biopolymers through nanotubes.

There is great interest in studying protein folding and dynamics in confined spaces because of their possible relevance to a variety of biological problems.<sup>1–7</sup> These include the fate of newly synthesized proteins as they exit the nearly 100 Å long and approximately cylindrical ribosome tunnel,<sup>1,4</sup> the effect of encapsulation of substrate proteins in the central cavity of the chaperonin GroEL,<sup>3</sup> and the translocation of peptides across pores.<sup>8–11</sup> Understanding the factors that determine the stability of confined proteins is also relevant in biotechnology applications.<sup>12</sup> The effect of being localized in the cylindrical tunnel of the ribosome, or the GroEL cavity, on peptide and protein stability is hard to predict because of the interplay of a number of energy and length scales.<sup>13–21</sup> They include the decrease, with respect to bulk, in conformational entropy of the ensemble of unfolded and native states, and the residue-dependent solvent-averaged interaction between the substrate protein with the interior of the confining pore. For example, the

ribosome tunnel is lined with RNA near the peptidyl transfer center (PTC) and proteins closer to the exit tunnel. As a result, the interaction of a nascent peptide with the walls of the tunnel varies as it traverses from the PTC toward the exit.<sup>6</sup> Thus, the formation of  $\alpha$ -helical structure in the tunnel, that is observed in experiments,<sup>4</sup> not only depends on the sequence but also on where the peptide is localized inside the ribosome.<sup>4,7</sup>

A number of factors contribute to the changes in the stability of a peptide upon confinement to a nanotube. The simplest scenario is the entropic stabilization mechanism (ESM),<sup>13–15,22</sup> which postulates that in confined spaces the number of allowed conformations is restricted compared to the bulk. As a result, the free energy change  $\Delta F_U$  of the denatured state ensemble (DSE) and the  $\Delta F_N$  of the native state ensemble (NSE) both increase. If the native state is not significantly altered in the confined space then  $\Delta F_U \gg \Delta F_N$ . Hence, confinement entropically stabilizes the native state relative to the DSE. The stabilization of polypeptide chains suggested by ESM holds good only when  $D$ , the diameter of the nanotube, exceeds a threshold value, because the entropy cost of confinement of the ordered ( $\alpha$ -helical) conformation is prohibitive when  $D$  is small.<sup>17</sup> If water mediated interactions involving proteins are altered by

\* Corresponding author. Phone: 301-405-4803. Fax: 301-314-9404.  
E-mail: thirum@glue.umd.edu.

† Institute for Physical Science and Technology, University of Maryland.

‡ National Heart Lung and Blood Institute.

§ University of Cincinnati.

|| Department of Chemistry and Biochemistry, University of Maryland.

**Table 1.** Models and Simulation Details

sequence	label	$\epsilon_{\text{HB}}^a$	$\epsilon_{\text{BB}}^b$	$D$ (Å)	time ( $\mu\text{s}$ ) <sup>c</sup>	$P_{\text{HB}}^d$
GDLDDLLKKLKDLLKG <sup>e</sup>	AS <sub>1</sub> <sup>f</sup>	0.00	2.125	25.8	2.0	0.17
	AS <sub>2</sub> <sup>g</sup>	1.75	2.125	all <sup>h</sup>	3.3	0.50
	AS <sub>3</sub> <sup>i</sup>	2.75	0.50	all	3.3	0.48
A <sub>16</sub>	PA	2.75	0.50	all	3.3	0.40
	PN	2.50	0.50	all	3.3	0.48

<sup>a</sup> The implicit hydrogen bonding energy in kilocalories per mole; see eq 6 in the Supporting Information. <sup>b</sup> The Lennard-Jones well-depth between hydrophobic residues in kilocalories per mole; see eq 5 in the Supporting Information. <sup>c</sup> The total simulation time per nanotube diameter. <sup>d</sup> The probability of being in the HB in bulk. <sup>e</sup> One letter code is used for amino acids. <sup>f</sup> Original parameter set of Guo and Thirumalai.<sup>36</sup> <sup>g</sup> Modified dihedral potential (see Table 1 in the Supporting Information) and  $V_{\text{HB}}$  term (see eq 6 in the Supporting Information). <sup>h</sup> The term all indicates that nanotubes with  $D = 35.3, 29.8, 25.8, 20.3, 17.6$ , and  $14.9$  Å were studied. <sup>i</sup> Same parameter set as AS<sub>2</sub> except  $\epsilon_{\text{BB}} = 0.5$  kcal/mol.

confinement then it may be possible for  $\Delta F_N > \Delta F_U$ .<sup>2,15,18,20,23</sup> In this case, the native state can be destabilized in nanotubes. More generally, if specific interactions between the polypeptide and the walls of the pore are relevant, as appears to be the case in certain regions of the ribosome tunnel, the diagram of states of a confined polypeptide or protein can be rich.<sup>24</sup>

Here, we study the changes in stabilities of a number of peptide sequences that form helices to varying extents in bulk. By varying  $D$ , the strength of interaction,  $\lambda$  (see eq 7 in the Supporting Information), between the hydrophobic residues and the carbon nanotube, and the polypeptide sequence, we show that an interplay of a number of factors determines the stability of helical states of peptides confined to nanotubes. We find that the helix is entropically stabilized when  $D$  is small and the interaction between peptides and the nanotube is weak. As  $\lambda$  increases, the peptide can adsorb onto the wall of the nanotube. Interestingly, adsorption results in stabilization of the helix for an amphiphilic sequence and destabilization for a polyalanine sequence. If the wall of the nanotube is decorated with patches that are “hydrophobic”, the helical stability can increase for the polyalanine. Thus, a very rich diagram of states of helix forming sequences is envisioned upon confinement in a nanotube.

**Methods.** In order to explore a wide range of possibilities we consider several helix forming sequences. The sequences are GDLDDLLKKLKDLLKG (an amphiphilic sequence denoted by AS),<sup>25,26</sup> polyasparagine N<sub>16</sub> (a polar sequence denoted PN),<sup>27,28</sup> and polyalanine A<sub>16</sub> (a hydrophobic sequence denoted PA).<sup>29</sup> Each sequence is 16 residues long, which is close to the average helix length of  $\sim 14$  found in globular proteins.<sup>30</sup> We use three variations of AS to probe the effects of varying the bulk peptide properties (the nature of the DSE and NSE) on confinement. The parameters of sequence AS<sub>1</sub> (see Table 1) renders the helical state unstable in the bulk ( $D \rightarrow \infty$ ). Sequences AS<sub>2</sub> and AS<sub>3</sub> are modeled so that they form stable helices in the bulk. The changes in the intrapeptide interactions (see Table 1 and the Supporting Information for details) between the hydrophobic residues in AS<sub>2</sub> and AS<sub>3</sub> accounts for differences in  $\epsilon_{\text{BB}}$  (eq 6 in the Supporting Information) that can arise by adding cosolvents (see the Supporting Information for details).

We use the Honeycutt–Thirumalai (HT)<sup>31</sup> model for the polypeptide chain. In the HT model, each amino-acid is represented by one bead located at the  $C_{\alpha}$ -carbon position. A three letter code is used to classify the twenty naturally occurring amino acids; L for hydrophilic residues, B for hydrophobic residues, and N for neutral residues. The potential energy of a conformation of a polypeptide with  $M$  residues, and coordinates  $r_i$  ( $i = 1, 2, \dots, M$ ) in the HT representation is  $V = V_B + V_A + V_D + V_{\text{NB}} + V_{\text{HB}}$ , where  $V_B$ ,  $V_A$ , and  $V_D$  are the bond-stretch, bond-angle, and the dihedral potentials respectively. The stability of the helices in the bulk can be altered by tuning the interaction,  $V_{\text{NB}}$ , between noncovalently linked beads, as well as the hydrogen bond potential  $V_{\text{HB}}$ . Details on the functional form and the parameters of the energy function are provided in the Supporting Information.

In order to enhance the sampling of the conformational space of the peptide, we use underdamped Langevin dynamics<sup>32</sup> with a friction coefficient of  $0.016$  ps<sup>-1</sup> and an integration timestep of 15 fs. Simulations are prepared and simulated in the NVT ensemble at 300 K using the CHARMM software package (version c32b2).<sup>33</sup>

**Helical Basin (HB).** A given peptide conformation is classified as helical using two order parameters. They are the end-to-end distance ( $R_{\text{ee}}$ ) and the number of helical triads ( $N_{\text{HT}}$ ). We define helical triads as three consecutive dihedral angles that are in the helical region ( $35^\circ \leq \phi \leq 75^\circ$ ). A polypeptide with 16 residues has a total of eleven helical triads. In a completely helical conformation  $N_{\text{HT}} = 11$ , while  $N_{\text{HT}} = 0$  corresponds to a completely random coil conformation. A conformation is deemed to be in the HB if  $21.25 < R_{\text{ee}} < 28.75$  Å and  $8 \leq N_{\text{HT}} \leq 11$ . The two order parameters  $R_{\text{ee}}$  and  $N_{\text{HT}}$  separate the helical and denatured basins into distinct regions (see the inset in Figure 1C).

**Results and Discussion.** For sequence AS<sub>1</sub>, the probability of being in the HB ( $P_{\text{HB}}$ ) is 0.17 in bulk. The values of  $P_{\text{HB}}$  for AS<sub>2</sub>, AS<sub>3</sub>, PA, and PN are between 0.40 and 0.50 in the bulk (Table 1).

**Helices are Entropically Stabilized in Narrow and Weakly Hydrophobic Nanotubes.** If the attractive interaction between the hydrophobic residues and the nanotube is weak ( $\lambda < 0.4$ ), then confinement enhances helix stability of all sequences provided  $D < D^*$ , where  $D^*$  depends on the sequence (Figure 1) and is greater than or equal to 20 Å for the sequences studied here. For example, when AS<sub>3</sub>, PA and PN are in a nanotube with  $D = 14.9$  Å, and  $\lambda = 0.01$ , the helix is stabilized by 0.71, 0.68, and 0.49 kcal/mol, respectively (computed using the data from Figure 1). The enhanced helix stability at  $D < D^*$  and  $\lambda < 0.4$  can be explained using polymer arguments,<sup>17</sup> from which it follows that when  $D$  is small enough the helical basin is entropically stabilized. Figure 1 shows that the helical content of AS<sub>3</sub> and PN increases for all  $D$ . While for AS<sub>2</sub> and PA,  $P_{\text{HB}}$  increases only below  $D < D^* \sim (20-22)$  Å. The sequence-dependent values of  $D^*$  are difficult to predict using polymer theory alone. Interestingly, for AS<sub>2</sub> and PA we find that  $P_{\text{HB}}$  changes nonmonotonically as  $D$  decreases (Figure 1A and B). Such a behavior is also mirrored in the variation of  $R_{\text{ee}}$  as  $D$  is

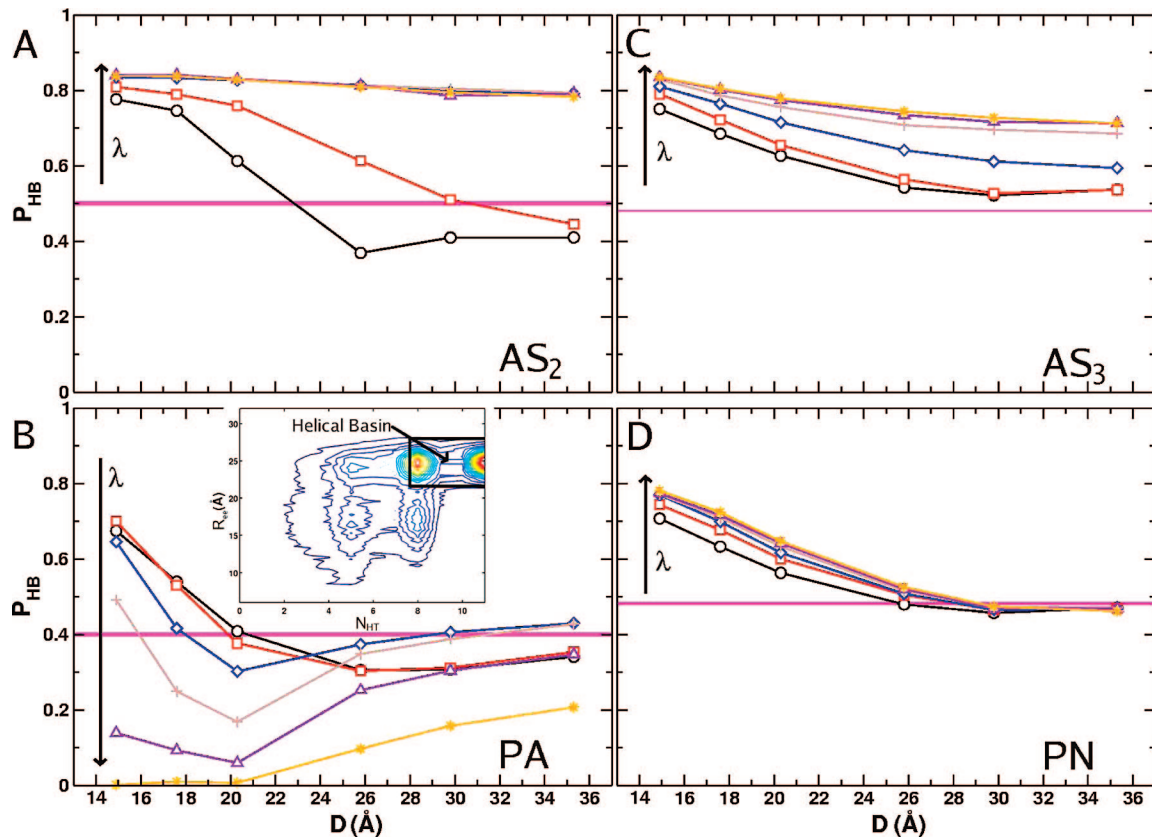


**Figure 1.** Probability of being in the HB as a function of nanotube diameter for the sequences AS<sub>2</sub> (A), PA (B), AS<sub>3</sub> (C), and PN (D) at various  $\lambda$  values ( $\lambda = 0.01$  (black circles), 0.1 (red squares), 0.3 (blue diamonds), 0.5 (brown plus signs), 0.7 (purple triangles), and 1.0 (orange stars)). The horizontal magenta colored line, in each graph, corresponds to the probability of being helical in bulk, and the width corresponds to the standard error of  $P_{\text{HB}}^{\text{B}}$ . We characterized a given peptide conformation as helical using two order parameters, the end-to-end distance ( $R_{\text{ee}}$ ), and the number of backbone dihedral angles that are helical (“helical triads”) (see the inset in panel C). A peptide conformation is helical if  $21.25 < R_{\text{ee}} < 28.75 \text{ \AA}$  and  $8 \leq N_{\text{HT}} \leq 11$ . The value of  $\lambda = 0.01$  in all panels.

changed (data not shown), in agreement with theoretical predictions.<sup>34</sup>

For small  $\lambda$  ( $\sim 0.01$ ), we expect that the effect of confinement can be described by the difference in entropy changes in the DSE and the HB. We estimate confinement-induced free energy changes using

$$\Delta\Delta G(D, \lambda \sim 0.01) \approx -T[k_B \ln(\alpha_{\text{HB}}(D)) - k_B \ln(\alpha_{\text{DSE}}(D))] \approx -T[\Delta S_{\text{HB}}(D) - \Delta S_{\text{DSE}}(D)] \quad (1)$$

where  $\Delta S_{\text{HB}}(D)$  and  $\Delta S_{\text{DSE}}(D)$  are the changes in entropy upon confinement of the helix and DSE, respectively. The volume fraction accessible to the HB ( $\alpha_{\text{HB}}(D)$ ) and DSE ( $\alpha_{\text{DSE}}(D)$ ), are calculated numerically using the Widom particle insertion method (see the Supporting Information for details). The similarity (Figure 2) in the values of  $\Delta\Delta G(D)$  computed using  $\alpha_{\text{HB}}(D)$  and  $\alpha_{\text{DSE}}(D)$  and that obtained directly from  $P_{\text{HB}}(D)$  (Figure 1) shows that the helix formed by AS<sub>3</sub> is entropically stabilized for all  $D$ . In contrast,  $\Delta S_{\text{DSE}}(D) > \Delta S_{\text{HB}}(D)$  for AS<sub>2</sub> and PA when  $D > D^* \sim 20 \text{ \AA}$  which leads to destabilization of the helix upon confinement. Thus, the differences in the intrapeptide interaction strength between sequences AS<sub>2</sub> and AS<sub>3</sub> can change the nature of the DSE and HB and can result in either helix stabilization (for AS<sub>3</sub>) or helix destabilization (for AS<sub>2</sub>) when  $D > 20 \text{ \AA}$ . The differing behavior of AS<sub>2</sub> ( $\epsilon_{\text{BB}}/k_B T \approx 3$ ) and AS<sub>3</sub> ( $\epsilon_{\text{BB}}/k_B T \approx 0.9$ ) shows that the nature of the conformations explored in the bulk affects confinement-induced

stability. In principle,  $\epsilon_{\text{BB}}$  can be altered in experiments by addition of cosolvents or by changing temperature.

#### Hydrophobic Residues Are Pinned to the Nanotube As $\lambda$ Increases.

We expect that increasing  $\lambda$  should result in sequences containing hydrophobic residues to adsorb onto the nanotube wall. The probability density of finding a residue  $i$  at a distance  $r_i$  from the long nanotube axis shows that all sequences sample the interior of the nanotube at  $\lambda = 0.01$  (Figure 3). As a result, we expect that confinement-induced helix stabilization should be largely determined by entropy considerations. However, as  $\lambda$  increases, sequences containing hydrophobic residues (PA, AS<sub>1</sub>, AS<sub>2</sub>, and AS<sub>3</sub>) can be pinned to the wall, as indicated by the greater probability density of peptide residues near the nanotube surface (Figure 3A and B). In the case of the amphiphilic sequence, the peptide sticks to the wall (Figure 3A) and forms a helix (Figure 1A and C). The spatial distribution of residues in the HB corresponds well with the probability density plotted for  $\lambda = 1.0$  (Figure 3A). The results in Figure 3, which show that hydrophobic residues are pinned to the wall, while polar residues are more likely to be sequestered in the interior of the nanotube, suggests that a “phase separation” occurs on the molecular length scale between hydrophobic and polar peptide residues.

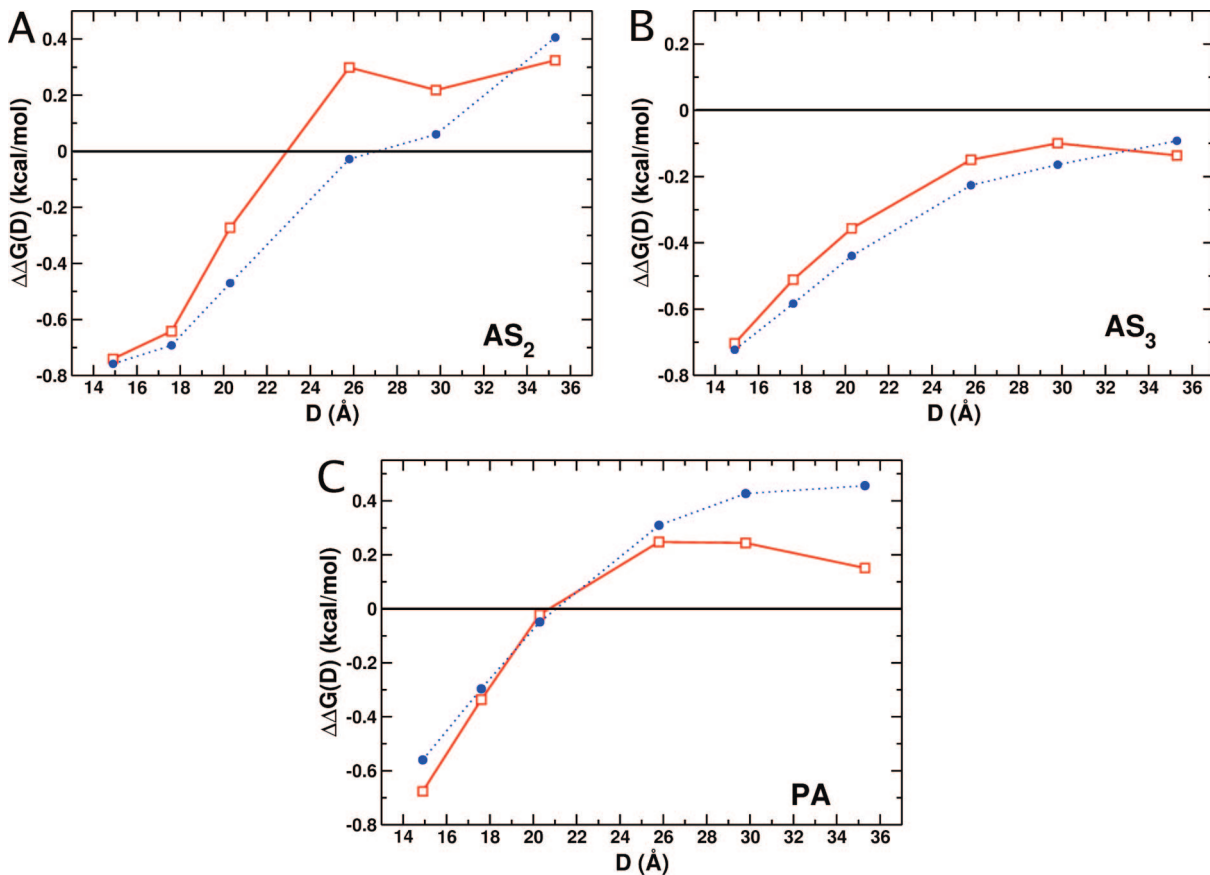


**Figure 2.** Change in free energy ( $\Delta\Delta G(D) = \Delta G(D) - \Delta G(B)$ ) of the HB, relative to the DSE, upon nanotube confinement as a function of  $D$ . The free energy difference in the bulk ( $D \rightarrow \infty$ ) is given by  $\Delta G(B)$ .  $\Delta\Delta G(D)$  computed from  $P_{\text{HB}}(D)$  ( $\Delta\Delta G(D) = -k_B T \ln\{[P_{\text{HB}}(D)P_{\text{HB}}^B]/[(1 - P_{\text{HB}}(D))(1 - P_{\text{HB}}^B)]\}$ ) and  $\alpha(D)$  (see eq 1) are shown as red squares and blue circles, respectively. Lines are to guide the eye. The results in panels A, B, and C are for AS<sub>2</sub>, AS<sub>3</sub>, and PA respectively.

The distribution functions in Figure 3 show that for an amphiphilic sequence, the stability of helices should be determined by the opposing tendency of hydrophobic residues to be pinned to the wall of the nanotube and the preference of the polar residues to be localized in the interior. Indeed, we find that for AS<sub>1</sub>, AS<sub>2</sub>, and AS<sub>3</sub>, the helical content increases as  $\lambda$  increases (Figure 4). The effect of increasing  $\lambda$  is most dramatic for AS<sub>1</sub> ( $\epsilon_{\text{BB}} = 0$ ), for which  $P_{\text{HB}}$  increases dramatically from below the bulk value of  $P_{\text{HB}}^B \approx 0.17$  (Figure 4A). For AS<sub>1</sub>, the helix is greatly stabilized by the favorable interactions between the hydrophobic residues and the nanotube. In the case of AS<sub>2</sub>, increasing  $\lambda$  maximizes the attractive interactions between B (hydrophobic) beads with the nanotube without compromising the intrapeptide BB interactions in the HB. Similarly,  $P_{\text{HB}}$  increases (Figure 4B) for AS<sub>3</sub> ( $\epsilon_{\text{BB}} = 0.5$  kcal/mol) as  $\lambda$  increases although the changes in  $P_{\text{HB}}$  occur over a wider range of  $\lambda$  compared to AS<sub>2</sub> ( $\epsilon_{\text{BB}} = 2.125$  kcal/mol) (Figure 4B).

When the amphiphilic sequence is in the HB, all of the hydrophobic residues are aligned on one side of the helix while the polar residues are exposed on the other side (Figure 3A). Thus, for all variations of AS, the HB is stabilized because it maximizes the hydrophobic interaction between the hydrophobic face of the helix and the hydrophobic surface of the nanotube. If the helical pitch ( $p$ ) is commensurate with

the distance between the carbon atoms ( $R_{\text{CC}}$ ) along the long axis of the nanotube, we expect that the interactions between the hydrophobic residues and the nanotube can be maximized without compromising the helical structure. Conversely, if  $p$  and  $R_{\text{CC}}$  are incommensurate it is likely that the helix may be denatured. Thus, besides the sequence, the relative positions of the hydrophobic residues in the helix are also important determinants of stability in a nanotube, especially as  $\lambda$  increases.

**Rich Phase Diagram of States of Polyalanine in a Carbon Nanotube.** The interplay between the strength of the hydrophobic interactions and the entropy of confinement results in a rich phase diagram in the  $(\lambda, D)$  plane for PA (Figure 5A). The stability of the HB decreases as  $\lambda$  increases as long as  $D < \sim 20$  Å (see points 1, 5, and 6 in Figure 5A). The effect is most dramatic in the narrowest tube ( $D = 14.9$  Å in Figure 5B) in which  $P_{\text{HB}}$  nearly vanishes as  $\lambda$  approaches unity. In larger nanotubes ( $D > 20$  Å),  $P_{\text{HB}}$  increases by about (7–10)% as  $\lambda$  increases from  $\lambda = 0.01$ , reaches a maximum at  $\lambda \sim 0.4$ , and then decreases upon further increase in  $\lambda$  (Figure 5B and see points 2, 3, and 4 in Figure 5A). This modest helix stabilization occurs because the peptide weakly binds to the wall of the nanotube as  $\lambda$  increases (Figures 3B and 5A, point 3), resulting in preferential alignment of the peptide along the long axis of the nanotube (Figure 5B point 3 and Figure 2A of the Supporting

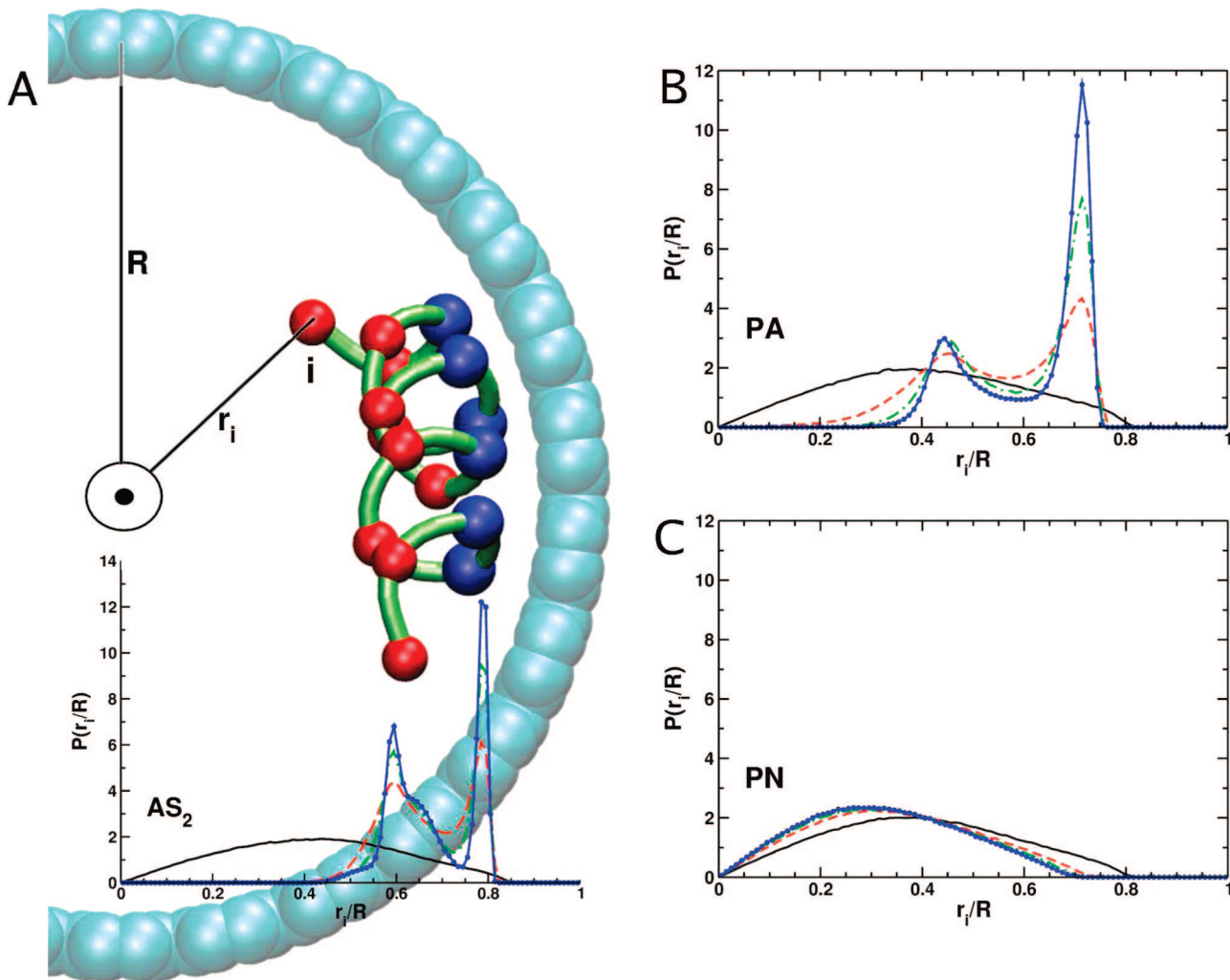


**Figure 3.** Probability density of finding a residue  $i$  at a distance  $r_i/R$  ( $R$ , the nanotube radius, is  $14.9 \text{ \AA}$  in panel A and  $12.9 \text{ \AA}$  in panels B and C) from the long nanotube axis at different  $\lambda$  values for  $AS_2$  (A), PA (B), and PN (C). Four different values of  $\lambda$  are plotted,  $\lambda = 0.01$  (solid black line), 0.3 (dashed red line), 0.7 (dash-dot green line), and 1.0 (solid blue line with circles). The image in the background of panel A is on the same scale as the graph overlaying it. The spatial distribution of the residues in the image correspond well with the probability density at  $\lambda = 1.0$ . In the image, hydrophobic residues are shown in blue and polar residues are in red.

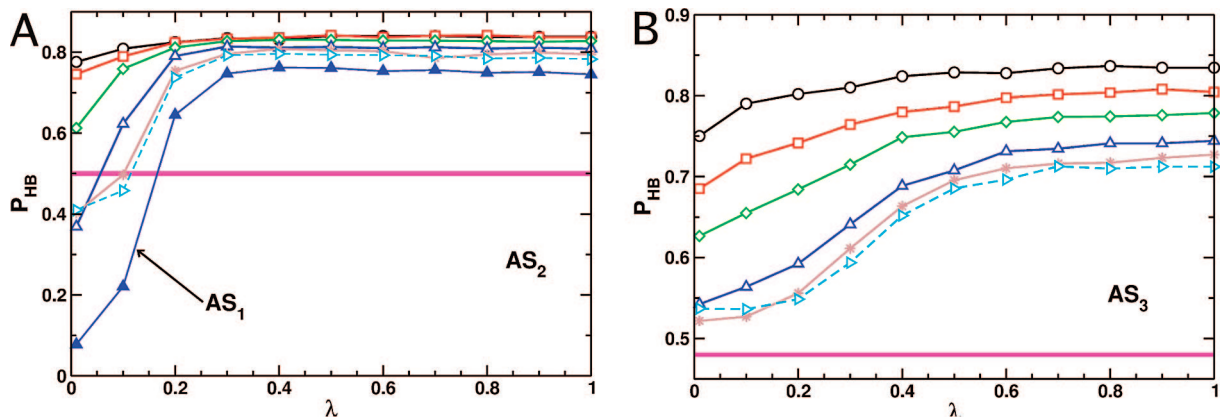


**Figure 4.** Probability of being in the HB as a function of  $\lambda$  in different diameter nanotubes for the three variations of the amphiphilic sequence. The graphs show that  $AS_1$ ,  $AS_2$ , and  $AS_3$  tend to be stabilized by increasing the strength of the hydrophobic interactions with the nanotube.  $P_{HB}$  versus  $\lambda$  is shown for the two amphiphilic sequences  $AS_2$  (A) and  $AS_3$  (B) for different nanotube diameters ( $D = 35.3 \text{ \AA}$  cyan triangles,  $29.8 \text{ \AA}$  brown stars,  $25.8 \text{ \AA}$  blue triangles,  $20.3 \text{ \AA}$  green diamonds,  $17.6 \text{ \AA}$  red squares, and  $14.9 \text{ \AA}$  black circles). Results for  $AS_1$  with  $D = 25.8 \text{ \AA}$  are shown as blue filled triangles in panel A.

Information). At  $\lambda \approx 0.4$  and  $D > 20 \text{ \AA}$ , the interaction with the nanotube is not strong enough to overcome the internal

peptide energies which favor the helix. As a result, the nanotube-peptide interactions are maximized when the

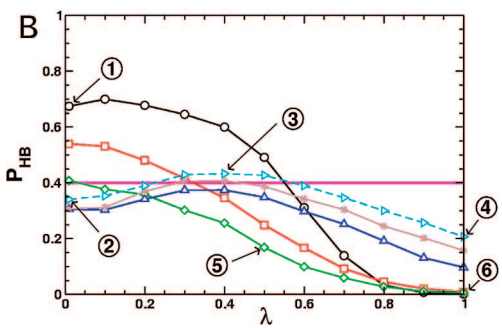
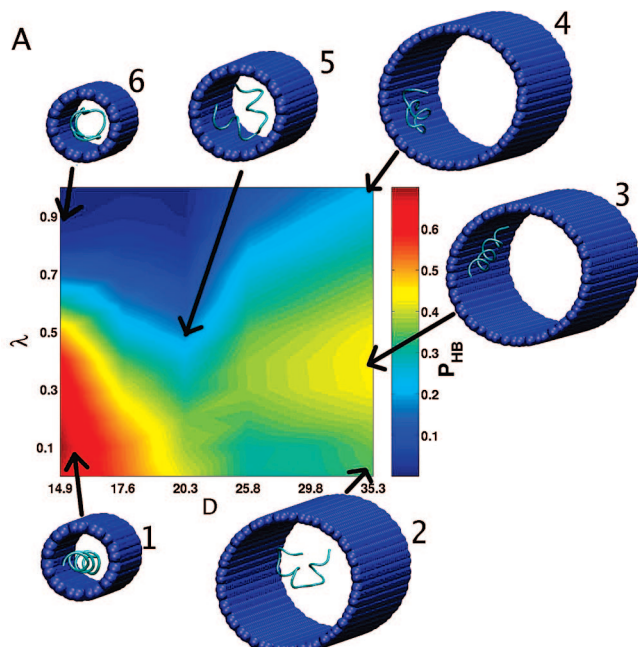


**Figure 5.** Probability of being in the HB as a function of  $D$  and  $\lambda$  for PA. (A) Phase diagram in the  $(\lambda, D)$  plane. Representative structures are shown in the images labeled 1–6. (B) Dependence of  $P_{HB}$  on  $\lambda$  for various values of  $D$ . See Figure 4 for an explanation of the symbols. The points labeled 1–6 correspond to the structures labeled in panel A.

peptide is in the HB. As  $\lambda$  is further increased, hydrophobic interactions with the wall cause the helical content to decrease (Figure 5B). In the largest nanotube ( $D \approx 35 \text{ \AA}$ ), as  $\lambda$  approaches unity,  $P_{HB}$  decreases because the peptide gets splayed out along the interior of the nanotube surface (Figure 5A, point 4). For nanotubes with  $D \approx 20 \text{ \AA}$ , increasing  $\lambda$  stabilizes a “broken” helix (Figure 5, point 5) that does not align along the long nanotube axis (Figure 2A in the Supporting Information), but instead binds to the nanotube perpendicular to the nanotube axis (Figure 2B in the Supporting Information). For the smallest diameter nanotubes, increasing  $\lambda$  stabilizes a coiled peptide that coats the interior surface of the nanotube (Figure 5A, point 6) but has no helical dihedral angles.

Taken together, these results show that the effect of varying the hydrophobic character of the nanotube on helix stability is subtle for the PA. For the largest nanotube diameters there is an optimal hydrophobic strength which stabilizes the helix modestly. For smaller nanotube diameters, divergent behavior is observed. Weakly hydrophobic nanotubes ( $\lambda < 0.4$ ) stabilize the helix as  $D$  gets smaller. In contrast, destabilization of the helix occurs when  $\lambda > 0.6$ .

**Hydrophobic Patches Lining the Nanotube Affect  $P_{HB}$  of PA.** To mimic the chemical heterogeneity of the groups in the ribosome tunnel, which has small hydrophobic patches from proteins (such as L4, L17, and L39 in the ribosome of eukaryotes<sup>4</sup> surrounded by hydrophilic patches from RNA),<sup>35</sup> we created different size hydrophobic patches that line the nanotube (Figure 6A). The desired heterogeneity is achieved by assigning hydrophilic character to subsets of nanotube atoms that run parallel to the long nanotube axis and hydrophobic behavior to the rest of the nanotube atoms (see the Methods section for details). With  $\lambda = 0.9$ , we vary the size of the hydrophobic patch. The fraction of hydrophobic surface area  $f_H$  varies from 0 to 1. Surprisingly, we find that the helical stability of PA, whose helical content is negligible at  $\lambda = 0.9$  and  $f_H = 1$  for all  $D$  (Figure 1), increases as  $f_H$

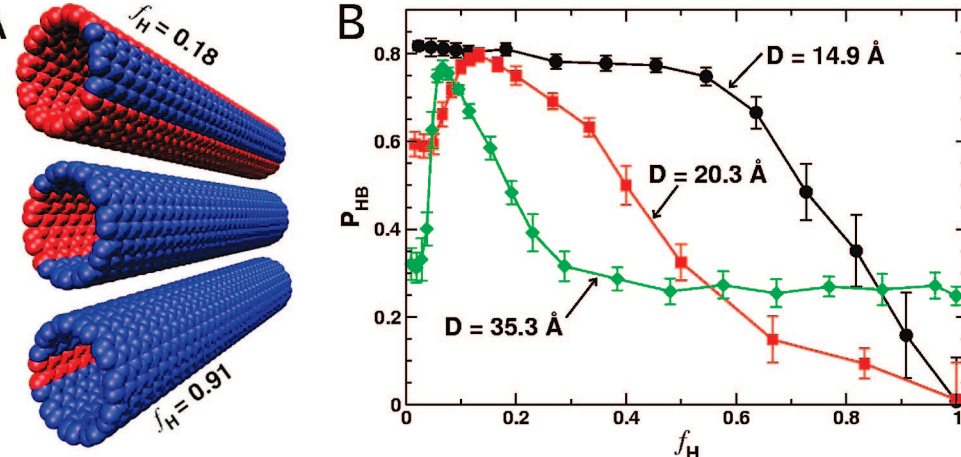


**Figure 6.** Changes in  $P_{HB}$  for PA in a chemically heterogeneous nanotube. (A) Size of the hydrophobic patch lining the nanotube (nanotube atoms with hydrophobic character are shown in blue, while those with hydrophilic character are shown in red). The value of  $D$  is  $14.9 \text{ \AA}$ , and the fraction of nanotube hydrophobic surface area,  $f_H$ , is 0.18, 0.73, and 0.91 for the top, middle, and bottom nanotubes. (B) Probability of being in the HB as a function of  $f_H$  with  $D = 14.9, 20.3$ , and  $35.3 \text{ \AA}$ , and  $\lambda = 0.9$ . For the smallest nanotube, a homogeneous hydrophobic environment ( $f_H = 1$ ) destabilizes the helix, while the smallest hydrophobic patches maximize helix stability. For larger  $D$ , there is an optimal hydrophobic patch size that maximizes helix stability.

decreases (Figure 6B). In the smallest nanotube ( $D = 14.9 \text{ \AA}$ ),  $P_{\text{HB}}$  increases monotonically as  $f_{\text{H}}$  decreases, with the smallest hydrophobic patch imparting the greatest helix stability. In larger nanotubes,  $P_{\text{HB}}$  as a function of  $f_{\text{H}}$  is nonmonotonic. Thus, there is an optimal  $f_{\text{H}}$ , between 0.08 and 0.15, in these larger nanotubes that maximizes  $P_{\text{HB}}$  for PA.

**Conclusions.** The effect of nanotube confinement on the stability of the helical states depends on the sequence, the tube diameter, and nanotube–peptide interactions as well as the chemical heterogeneity of the nanotube. The remarkably complex behavior of peptides in nanotubes illustrates that it is possible to control confinement-induced helix stability by altering a number of variables. The substantial diversity in the stability as a function of ( $D, \lambda$ ), even for a specific sequence (Figure 5A), shows that solvent-mediated peptide-nanotube interactions (parametrized by  $\lambda$ ) can either stabilize or destabilize the HB depending on  $D$ . Our results show that it would be erroneous to draw general conclusions<sup>20</sup> based on the study of a single sequence in a nanotube with various values of  $D$ .

A key prediction of this study is that confinement-induced helix stability can be dramatically altered by varying the intrapeptide interactions or by changing the interaction strength between the peptide and the nanotube. The changes in the stability of the HB of the amphiphilic sequence (AS<sub>1</sub>, AS<sub>2</sub>, and AS<sub>3</sub>) most vividly illustrate the effects of  $\lambda$ ,  $\epsilon_{\text{BB}}$ , and  $D$  (Figure 1). The variations in  $\epsilon_{\text{HB}}$  and  $\epsilon_{\text{BB}}$ , which distinguish AS<sub>1</sub>, AS<sub>2</sub>, and AS<sub>3</sub>, can be realized by varying cosolvent conditions. The differences in their stabilities upon confinement in AS<sub>1</sub>, AS<sub>2</sub>, and AS<sub>3</sub> is due to substantial changes in the DSE. The finding that the stability of a polyalanine sequence can be greatly altered by changing  $\lambda$  and  $D$  (see Figure 5A) can be experimentally tested. The changes in  $\lambda$  can be achieved by varying the solvent density in the nanotube.

A prediction of plausible relevance to peptide folding in the ribosome is the demonstration that helix stability also depends strongly on the size of the hydrophobic patch lining the nanotube. If the entire interior of the nanotube is hydrophobic ( $f_{\text{H}} = 1$ ), the HB of the polyalanine peptide is completely destabilized when the interaction between the peptide and the nanotube is  $\lambda = 0.9$ . However, as the patch takes up a smaller percentage of the surface area of the nanotube, the stability of the polyalanine helix increases. In the nanotube diameter range comparable to the ribosome tunnel ( $D \approx 15 \text{ \AA}$ ), we find that the smallest size hydrophobic patches maximizes the helix stability. As a result, we predict that helix stability can increase in regions of the ribosome tunnel where small hydrophobic patches exist. Clearly, the extent of stabilization in the ribosome tunnel will depend on the sequence.

**Acknowledgment.** The authors thank Vincent Crespi for a computer program to generate atomic coordinates of carbon

nanotubes. This work was supported in part by grants from the NSF (05-14056) to D.T., Scientific Development Grant from the American Heart Association to G.S., the Intramural Research Program of the NIH, National Heart Lung and Blood Institute, to B.R.B., and a NIH GPP Biophysics Fellowship to E.P.O.

**Supporting Information Available:** Computational Methods. This material is available free of charge via the Internet at <http://pubs.acs.org>.

## References

- Nissen, P.; Hansen, J.; Ban, N.; Moore, P. B.; Steitz, T. A. *Science* **2001**, *289*, 920–929.
- Eggers, D. K.; Valentine, J. S. *Protein Sci.* **2001**, *10*, 250–261.
- Thirumalai, D.; Lorimer, G. H. *Ann. Rev. Biophys. Biomol. Struct.* **2001**, *30*, 245–269.
- Woolhead, C. A.; McCormick, P. J.; Johnson, A. E. *Cell* **2004**, *116*, 725–736.
- Groll, M.; Bochtler, M.; Brandstetter, H.; Clausen, T.; Huber, R. *ChemBioChem* **2005**, *6*, 222–256.
- Lu, J.; Deutsch, C. *Biochem.* **2005**, *44*, 8230–8243.
- Lu, J.; Deutsch, C. *Nat. Struct. Molec. Biol.* **2005**, *12*, 1123–1129.
- Hannah, S. C.; Wagner, R.; Sveshnikova, R.; Harrer, R.; Soll, J. *Biophys. J.* **2002**, *83*, 899–911.
- Muro, C.; Grigoriev, S. M.; Pietkiewicz, D.; Kinnally, K. W.; Campo, M. L. *Biophys. J.* **2003**, *84*, 2981–2989.
- Hessa, T.; Kim, H.; Bihlmaier, K.; Lundin, C.; Boekel, J.; erson, H.; Nilsson, I.; White, S. H.; voh Heijne, G. *Nature* **2005**, *433*, 377–381.
- Mohammad, M. M.; Prakash, S.; Matouschek, A.; Movileanu, L. *J. Am. Chem. Soc.* **2008**, *130*, 4081–4088.
- Dekker, C. *Nat. Nano.* **2007**, *2*, 209–215.
- Betancourt, M. R.; Thirumalai, D. *J. Mol. Biol.* **1999**, *287*, 627–644.
- Zhou, H. X.; Dill, K. A. *Biochemistry* **2001**, *40*, 11289–11293.
- Klimov, D. K.; Newfield, D.; Thirumalai, D. *Proc. Natl. Acad. Sci. USA* **2002**, *99*, 8019–8024.
- Baumketner, A.; Jewett, A.; Shea, J. E. *J. Mol. Biol.* **2003**, *332*, 701–713.
- Ziv, G.; Haran, G.; Thirumalai, D. *Proc. Natl. Acad. Sci. USA* **2005**, *102*, 18956–18961.
- Cheung, M. S.; Klimov, D.; Thirumalai, D. *Proc. Natl. Acad. Sci. USA* **2005**, *102*, 4753–4758.
- Cheung, M. S.; Thirumalai, D. *J. Mol. Biol.* **2006**, *357*, 632–643.
- Sorin, E. J.; Pande, V. S. *J. Am. Chem. Soc.* **2006**, *128*, 6316–6317.
- Elcock, A. H. *PLOS Comp. Biol.* **2006**, *2*, 824–841.
- Minton, A. P. *Biophys. J.* **1992**, *63*, 1090–1100.
- Zhou, H. X. *J. Chem. Phys.* **2007**, *127*, 245101.
- Degrado, W. F.; Lear, J. D. *J. Am. Chem. Soc.* **1985**, *107*, 7684–7689.
- Ho, S. P.; Degrado, W. F. *J. Am. Chem. Soc.* **1987**, *109*, 6751–6758.
- Xiong, H.; Buckwalter, B. L.; Shieh, H. M.; Hecht, M. H. *Proc. Natl. Acad. Sci. USA* **1995**, *92*, 6349–6353.
- Ziegler, J.; Sticht, H.; Marx, U. C.; Muller, W.; Rosch, P.; Schwarzsinger, S. *J. Biol. Chem.* **2003**, *278*, 50175–50181.
- Dima, R. I.; Thirumalai, D. *Proc. Natl. Acad. Sci. USA* **2004**, *101*, 15335–15340.
- Williams, S.; Causgrove, T. P.; Gilman, R.; Fang, K. S.; Callender, R. H.; Woodruff, W. H.; Dyer, R. B. *Biochemistry* **1996**, *35*, 691–697.
- Kumar, S.; Bansal, M. *Biophys. J.* **1998**, *75*, 1935–1944.
- Honeycutt, J. D.; Thirumalai, D. *Proc. Natl. Acad. Sci. USA* **1990**, *87*, 3526–3529.
- Veitschans, T.; Klimov, D.; Thirumalai, D. *Fold. Des.* **1997**, *2*, 1–22.
- Brooks, B. R.; Brucolieri, R. E.; Olafson, B. D.; States, D. J.; Swaminathan, S.; Karplus, M. *J. Comput. Chem.* **1983**, *4*, 187–217.
- Morrison, G.; Thirumalai, D. *J. Chem. Phys.* **2005**, *122*, 194907.
- Voss, N. R.; Gerstein, M.; Steitz, T. A.; Moore, P. B. *J. Mol. Biol.* **2006**, *360*, 893–906.
- Guo, Z.; Thirumalai, D. *J. Mol. Biol.* **1996**, *263*, 323–343.

NL8019328